

Electric Susceptibility of Sodium-Doped Water Clusters by Beam Deflection

Álvaro Carrera, Marcos Mobbili, and Ernesto Marceca*

INQUIMAE-DQIAQF, Facultad de Ciencias Exactas y Naturales, Universidad de Buenos Aires, Ciudad Universitaria, Pabellón II, Buenos Aires, Argentina

Received: October 23, 2008; Revised Manuscript Received: January 8, 2009

The electric susceptibility of neutral sodium-doped water clusters $\text{Na}(\text{H}_2\text{O})_N$, $N = 6\text{--}33$, was determined by beam electric deflection. The clusters behave as polarizable particles; their intensity profiles exhibit global shifts toward the high-field region without the occurrence of broadening. In the conditions of the experiment, sodium–water clusters have a “floppy” structure and hence the electric susceptibility presents both electronic and orientational terms. Measured susceptibilities are somewhat higher than those of pure water clusters, and the contribution per water molecule is similar for both cluster types.

1. Introduction

Electric deflection (ED) of highly collimated molecular beams in a static electric field gradient is a well-established method^{1,2} to study the electric properties of molecules, small molecular complexes, and different type of clusters with metallic, covalent, and ionic structures. The particle’s static polarizability and dipole moment can be deduced from the analysis of the beam intensity profile, measured in the direction of the field gradient. Furthermore, as we will see later, ED profiles are very sensitive to whether the particle is rigid or not, and this effect has been used as an excellent experimental criterion to characterize the structure as being flexible and “floppy”.^{3,4}

Very recently, the polarity of molecular clusters $(\text{H}_2\text{O})_N$, $N = 3\text{--}18$, was investigated by Moro et al.⁵ using this technique. The authors found that water clusters present a floppy structure due to isomerization dynamics, and they measured average permanent dipole moments exceeding 1 D for the aggregates. A question arises whether the addition of a species with a strong dipole moment into a water cluster would produce a marked effect on its electric properties, thereby increasing significantly the cluster polarity or, on the other hand, if the local field generated by the embedded species will be mostly screened by the solute–solvent interactions.

In this work we have attached a sodium atom to preformed water clusters and carried out ED measurements on the resulting clusters $\text{Na}(\text{H}_2\text{O})_N$, $N = 6\text{--}33$. Experimental^{6–8} and theoretical^{9–13} work done on sodium–water clusters indicates that for $N > 4$ the 3s electron detaches from the sodium core, and the resulting $\text{Na}^+ - \{e^-\}$ species is stabilized by the solvent structure, namely the H-bonding network is distorted and water molecules reorient to accommodate the cation–electron pair. We will show that in the conditions of the experiment sodium–water clusters are nonrigid, and they possess size-dependent permanent dipole moments with average values higher than those found previously for pure water clusters. However, despite the presence of a charge-separated species in the cluster, the contribution to the electric susceptibility per water molecule is similar to that in pure water clusters.⁵ Finally, we will compare the experimental results with ab initio calculations of permanent dipole moments and electronic polarizabilities.

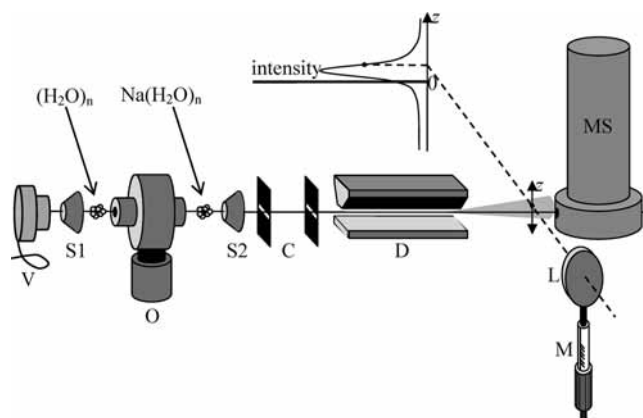


Figure 1. Scheme of the molecular beam apparatus: solenoid-driven valve, V; skimmers, S1 and S2; sodium oven, O; collimation slits, C; deflection electrodes, D; focusing lens, L; motor stage for scanning the ionization spot in the z axis, M; mass spectrometer, MS.

2. Methods

2.1. Experimental Setup. A scheme of the molecular beam apparatus employed in the ED measurements is presented in Figure 1. Sodium–water clusters were prepared by using a pickup arrangement.^{14,15} In the first stage, water clusters are generated by supersonic expansion of water-saturated helium at room temperature and 2 bar of pressure. The exit hole of a pulsed solenoid-driven valve (V) was used as a nozzle 400 μm in diameter and 2 mm in length. Having skimmed the beam to a diameter of 0.5 mm (S1), the clusters go through an oven (O) containing sodium vapor in equilibrium with the liquid metal at 230 °C. Sodium-doped water clusters formed by the collisions between sodium atoms and water clusters⁷ are stabilized by subsequent evaporation of 2 or 3 water molecules.¹⁶

By using two externally controlled slits (C) separated by a distance of 1000 mm, the beam is collimated to a height of 200 μm (z coordinate in the figure) and a width of 2000 μm . A few centimeters downstream, sodium–water clusters reach the deflection electrodes (D), designed according to a “two wire” field geometry¹⁷ to produce a constant z -field gradient at the beam position. In this configuration, the z -components of the field, F_z , and the field gradient, $\nabla_z F$, are proportional to the applied voltage, V . In this work, we have applied field strengths up to $F_z = 13.6$ kV/mm, which corresponds to $\nabla_z F = 3.3$ kV/

* Corresponding author. E-mail: marceca@qi.fcen.uba.ar.

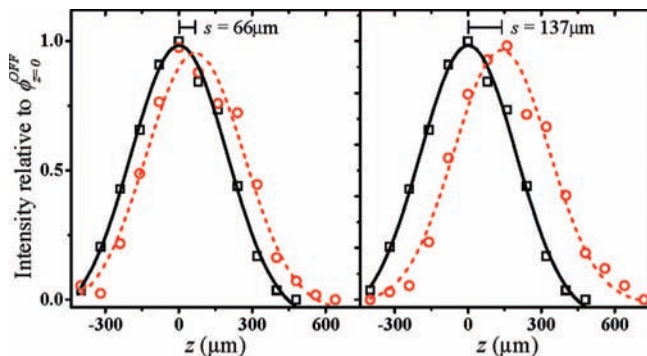


Figure 2. Effect of the electric field on the intensity profiles of $\text{Na}(\text{H}_2\text{O})_{17}$ clusters. Left panel: \square , field-off profile; \circ , $V = 15$ kV ($F_z = 10.2$ kV/mm, $\nabla F_z = 2.5$ kV/mm²). Right panel: \square , field-off profile; \circ , $V = 20$ kV ($F_z = 13.6$ kV/mm, $\nabla F_z = 3.3$ kV/mm²). The global shift of the intensity pattern is given by the value s .

mm². About half a meter downstream from the deflector, sodium–water clusters are photoionized by using a single 266 nm photon (fourth harmonic of a 1 mJ/pulse nanosecond Nd:YAG laser); it is known^{7,14} that in this process the photoelectron carries most of the excess energy and $\text{Na}(\text{H}_2\text{O})_N^+$ ions exhibit no fragmentation. The UV laser probes a small region of the beam (100 μm in the z direction) by means of a cylindrical lens (L). The collected ion yield is mass-analyzed by using a pulsed linear time-of-flight spectrometer (MS) operated under Wiley–McLaren conditions, and the intensity of the observed mass peaks is used to determine the cluster-size distribution at the ionization spot. A very clean mass spectrum is obtained by setting a delayed ion extraction pulse; this takes advantage of the higher propagation velocities of the beam cluster ions in comparison with background ions.

Size-selective ED studies involve the determination of the intensity profile for each cluster size (mass channel). This is achieved by collecting several mass spectra at different z -positions of the ionization spot (see the data points in Figure 2). To do this, the lens is driven with a precision linear motor stage (M) moving in steps along the z coordinate, alternating field-on and field-off scans. The detection efficiency in our setup showed no dependence with the position of the ionization spot within $z = \pm 1.5$ mm from the beam center.

The propagation speed of the clusters, v_y , was determined by using the following procedure: (i) 900 mm upstream from the MS, a synchronized fast rotating wire interrupts the beam for about 10 μs and (ii) we measure the time elapsed before the resulting intensity drop is detected in the MS. In the conditions of the experiment, we determined for v_y a value of 1580 ± 40 m/s. Within the accuracy of the method, no velocity spread was found at the front of the supersonic beam pulse.

The deflection unit and the skimmers are positioned along the y axis by using a telescope; after that, the alignment of each collimation slit is done by performing z -scans until a perfectly symmetric field-off profile is obtained.

2.2. Electric Deflection. For a particle of mass m propagating with a speed v_y , the deviation caused by the field along z is given by the equation:

$$d_z = \frac{C}{mv_y^2} \nabla_z F \langle \mu_z \rangle \quad (1)$$

where C is a geometrical constant of the apparatus¹⁷ and $\langle \mu_z \rangle$ represents the time-averaged z -projection of the dipole moment

evaluated during the transit time across the deflection electrodes. The constant C was determined from the beam deviation of nonpolar p -xylene molecules, whose polarizability value is known;¹⁸ two-photon ionization of p -xylene was achieved by increasing the laser power to 10 mJ/pulse.

If the system has a permanent dipole, μ_0 , and the rotational motion is uncoupled from vibrations, the value of $\langle \mu_z \rangle$ can be evaluated by using the theory of dipolar rigid rotors in electric fields for spherical,¹⁹ linear,^{20,21} symmetric,^{22,23} and asymmetric^{24,25} bodies. The overall intensity profile originates in distinct individual deviations $\{d_z\}$ corresponding to each accessible rotational state; this normally causes a substantial broadening of the beam profile that may be symmetrical^{22,26} or asymmetrical^{27,28} with respect to the z coordinate.

When coupling to vibrational modes cannot be disregarded, intramolecular motion affects the projection of the particle's dipole along z , and a simple formulation for $\langle \mu_z \rangle$ is generally no longer accessible. However, in the limiting case where the instantaneous dipole moments orient on the electric field's axis according to a canonical distribution, the Langevin–Debye linear response theory provides a useful expression for $\langle \mu_z \rangle$ given by²⁹

$$\langle \mu_z \rangle = \left(\alpha + \frac{\langle \mu_0^2 \rangle}{3k_B T} \right) F_z \quad (2)$$

where α represents the static electronic polarizability, $\langle \mu_0^2 \rangle$ is the average value of the squared magnitude of the system's dipole, and T is the cluster's internal temperature. In eq 2, the factor in parentheses corresponds to the electric susceptibility of the system, χ . The susceptibility acts as an effective polarizability,⁵ where a term considering the dipole orientation is added to the electronic component; the system behaves as a polarizable particle. In this regime, the value $\langle \mu_z \rangle$ is the same for all particles and therefore each one of them deviate to higher fields ($z > 0$) by the same amount; as a result, no beam broadening is observed. Nevertheless, the profile exhibits a global shift, s , to the right given by

$$s = \frac{C}{mv_y} \chi F_z \nabla_z F \quad (3)$$

This behavior has been observed in ED studies of relatively large molecules^{4,30} or molecular complexes^{3,31} having activated internal modes, and it was also found in clusters that go through isomerizations or fluctuations in the time scale of the experiments;^{5,19} in such cases, the system's structure is referred to as “floppy”. For a field geometry like that used in ED experiments, it can be deduced from eq 3 that the Langevin–Debye theory can be applied when the shift measured in the experiment shows a linear dependence with V^2 .

2.3. Calculations. The GAUSSIAN 98³² package was employed to calculate the permanent electric dipole and electronic polarizability of several isomers of clusters $\text{Na}(\text{H}_2\text{O})_8$ and $\text{Na}(\text{H}_2\text{O})_{20}$. The computation was based on density functional theory (DFT) performed at the BP86 level on optimized structures determined by Schulz et al.⁷ and Buck et al.,¹³ and using the Sadlej basis set³³ that is known to be specially designed for accurate calculation of polarizability. To test the functional employed to treat the electronic exchange–correlation, we considered the following: (a) the static electronic polarizability calculated for the sodium atom (22.81 \AA^3) was found in acceptable agreement with the corresponding experimental

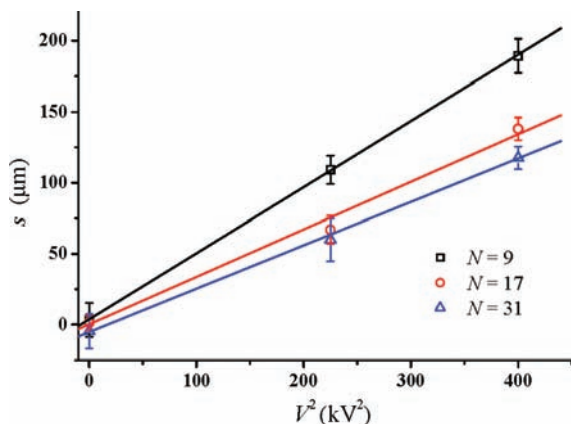


Figure 3. Profile shift of $\text{Na}(\text{H}_2\text{O})_N$, $N = 9, 17,$ and 31 , as a function of the squared applied voltage. Error bars were derived from the fitting procedure.

measurement (24.11 \AA^3)³⁴ and (b) the polarizability computed for the “cage” water hexamer (8.85 \AA^3) compares reasonably well with previous DFT calculations –(i) B3LYP functional/6-31++G(d,p) basis set (7.75 \AA^3),³⁵ (ii) B3PW91 functional/6-31++G(d,p) basis set (7.59 \AA^3),³⁵ (iii) B3LYP functional/Sadlej basis set (8.59 \AA^3),³⁶ and (iv) DFT-GGA/Gaussian basis set (9.42 \AA^3).³⁷

3. Results and Discussion

In the conditions of the experiment, the mass spectra showed a single series of $\text{Na}(\text{H}_2\text{O})_N$ clusters, with $N = 6\text{--}33$ and $N \approx 20$ at the maximum of the size distribution. The effect of the electric field on the intensity profile of the clusters evidence a total absence of broadening and an overall shift of the pattern toward the high-field region. As an example, in Figure 2 we show how the field-off profile (squares) of the cluster $\text{Na}(\text{H}_2\text{O})_{17}$ is gradually shifted to the right (circles) by increasing the voltage applied between the electrodes. The magnitude of the shift is calculated by fitting the data by using Gaussian curves, which represent adequately the measured profiles (see Figure 2). Independently of the size of the cluster, s was found to depend linearly on V^2 as shown in Figure 3 for three representative clusters ($N = 9, 17,$ and 31). As mentioned before, in terms of the Langevin-Debye formulation, the absence of broadening and the appearance of global shifts in polar systems is an indication of a fluctuating floppy structure. Sodium–water clusters are expected to be polar because the charge separation generated when the $3s$ electron is detached from the sodium atom might not be totally screened by the solvent structure. In fact, we have calculated large permanent dipole moments for several optimized structures^{7,13} of clusters $\text{Na}(\text{H}_2\text{O})_8$ and $\text{Na}(\text{H}_2\text{O})_{20}$; the corresponding values of μ_0 are listed in Table 1. With this in mind, the evidence collected in the ED studies clearly confirms that in our conditions the structure of sodium–water clusters is nonrigid, meaning that it undergoes a permanent interconversion among different isomeric species.

The electric susceptibility of the clusters was determined by replacing the measured values of s in eq 3. The results are plotted in Figure 4 as a function of the number of water molecules in the cluster; the χ values range from $144 \pm 13 \text{ \AA}^3$ for $N = 6$ to $326 \pm 36 \text{ \AA}^3$ for $N = 33$. At this time, we can use again the available structures^{7,13} for the clusters $\text{Na}(\text{H}_2\text{O})_8$ and $\text{Na}(\text{H}_2\text{O})_{20}$ and compute the contribution of the electronic polarizability (tabulated values of α in Table 1). We observed that the magnitude of α (averaged for the available isomers)

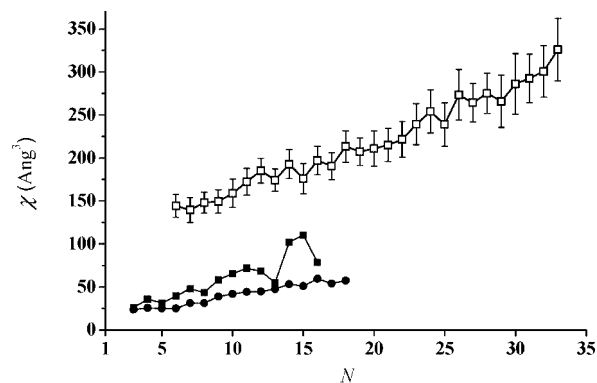


Figure 4. Electric susceptibility as a function of the number of water molecules in the cluster: \square , $\text{Na}(\text{H}_2\text{O})_N$ (this work); \bullet , $(\text{H}_2\text{O})_N$ (ref 5, neat water expansion); \blacksquare , $(\text{H}_2\text{O})_N$ (ref 5, water–He expansion). Error bars were derived from propagating errors corresponding to fitting procedure, determination of ν_s , and C .

TABLE 1: Calculated Electronic Polarizability (α) and Permanent Dipole Moment (μ_0) of Different Isomers of Clusters $\text{Na}(\text{H}_2\text{O})_8$ and $\text{Na}(\text{H}_2\text{O})_{20}$

isomer	$\text{Na}(\text{H}_2\text{O})_8$						$\text{Na}(\text{H}_2\text{O})_{20}$			
	A ^a	B ^a	C ^a	D ^a	W8a ^b	W8b ^b	A ^a	B ^a	C ^a	D ^a
α (\AA^3)	80.7	76.9	74.5	83.5	59.3	71.2	71.9	69.9	72.0	75.3
μ_0 (D)	3.9	3.6	2.5	4.2	2.9	1.6	6.1	9.3	6.9	5.3

^a Isomer structure given in ref 13. ^b Isomer structure given in ref 7.

represents only a fraction of the measured susceptibility: 50% for $N = 8$ ($\chi = 148 \pm 12 \text{ \AA}^3$) and 35% for $N = 20$ ($\chi = 211 \pm 20 \text{ \AA}^3$); the difference corresponds to the contribution of the fluctuating cluster-dipole on the susceptibility. The approximately linear increase of χ with the number of water molecules in the cluster, illustrated in Figure 4, implies that in this cluster-size range each added H_2O contributes nearly independently to the cluster dipole.

The average magnitude of the permanent dipole moment of the clusters can be estimated by introducing in eq 3 the values corresponding to the measured susceptibility and the calculated electronic polarizability. Since the cluster temperature is primary established in the pick-up/evaporation process, we used the evaporative ensemble theory³⁸ applied to aqueous clusters to estimate T in eq 3. The model predicts a temperature of 200 K, in agreement with the estimation done in previous work⁷ on $\text{Na}(\text{H}_2\text{O})_N$ aggregates prepared by using a pick-up arrangement.

The resulting values of μ_0 corresponding to $T = 200$ K are 2.5 ± 0.4 D for $N = 8$ and 3.4 ± 0.3 D for $N = 20$, where the uncertainties take into account the experimental error in the determination of χ and the variation of the calculated values of α for the different isomers. We found that fluctuation-averaged μ_0 derived from the experiment cannot be easily compared with the calculated values shown in Table 1 because of the strong dependence of this magnitude with the isomeric structure.

As mentioned before, pure water clusters $(\text{H}_2\text{O})_N$ were also described as nonrigid polar structures by Moro et al.⁵ The susceptibility measurements performed on this system by ED were included in Figure 4 for comparison. The χ -values of sodium–water clusters are found about 100 \AA^3 larger than those corresponding to He-seeded pure water clusters, and the difference is approximately independent of the cluster size. We will show that the observed difference is not only due to the expected bigger electronic polarizability of sodium-doped clusters, but also due to their larger cluster-dipoles. In the case of pure water clusters, it was shown³⁵ that each H_2O monomer

contributes with $\sim 1.3 \text{ \AA}^3$ to α , and this corresponds to a polarizability of about 10 \AA^3 for $N = 8$ and 26 \AA^3 for $N = 20$. On the other hand, the presence of the delocalized electron in sodium-doped clusters is reflected in a larger value of α ; for instance, the isomers listed in Table 1 have average α -values of 73 \AA^3 for $\text{Na}(\text{H}_2\text{O})_8$, and 72 \AA^3 for $\text{Na}(\text{H}_2\text{O})_{20}$. Such polarizability enhancement results are insufficient to explain the increment observed in the susceptibility of sodium-doped clusters, and this suggests that they must have a higher dipole moment; as an example, the fluctuation-averaged μ_0 determined⁵ for $(\text{H}_2\text{O})_8$ by ED under similar conditions is only about 1.3 D , a much lower value than that estimated by us for $\text{Na}(\text{H}_2\text{O})_8$.

Finally, despite the enormous electronic structure differences between sodium-doped and pure water clusters, we see that both systems exhibit a surprisingly similar dependence of χ with N in the studied cluster-size range. In accordance to the description done on sodium–water clusters,^{9,39} where about 4 water molecules form a tight solvation structure around the alkali ion leaving the 3s electron delocalized outside the cavity, the cluster-size range covered in this study concerns the behavior beyond the first solvation shell. Being far from the cation–electron moiety, it is reasonable to expect that the size dependence of the electric susceptibility becomes insensitive to the presence of sodium in the cluster.

4. Conclusions

We performed electric deflection measurements on a beam of sodium-doped aqueous clusters $\text{Na}(\text{H}_2\text{O})_N$, with $N = 6\text{--}33$. Within this range, the clusters behave as polarizable particles, namely the intensity profiles exhibit global shifts toward the high-field region without the occurrence of broadening. The magnitude of the shifts was found to exceed largely those calculated exclusively considering the electronic polarizability of the cluster; this fact together with the lack of profile broadening are clear indications that the clusters formed in the experiment have a floppy structure. The intramolecular motion will hence be coupled to the cluster rotation, allowing a partial alignment of the cluster dipole in the external field. This contribution to the electric susceptibility of the cluster was visualized as an orientational polarizability term.^{2,30}

According to our measurements, the magnitude of the electric susceptibility of sodium–water clusters is, as might be expected, somewhat higher than that corresponding to pure water clusters. However, we have observed the same contribution per water molecule to χ in both cluster types.

Acknowledgment. We are grateful for partial economic support given by the Volkswagen Stiftung, UBACyT X-330, and CONICET PIP-5228. E.M. is a member of the Carrera del Investigador, CONICET (Argentina); A.C. and M.M. thank CONICET (Argentina) for doctoral fellowships. We also thank K. Hashimoto, B. Gao, and Z. Liu for providing us the optimized structures of the cluster isomers used in Table 1.

References and Notes

- (1) Broyer, M.; Antoine, R.; Benichou, E.; Compagnon, I.; Dugourd, Ph. *C. R. Phys.* **2002**, *3*, 301, and references cited therein.
- (2) Broyer, M.; Antoine, R.; Compagnon, I.; Rayane, D.; Dugourd, Ph. *Phys. Scr.* **2007**, *76*, C135, and references cited therein.

- (3) Compagnon, I.; Antoine, R.; Rayane, D.; Broyer, M.; Dugourd, Ph. *Phys. Rev. Lett.* **2002**, *89*, 253001.
- (4) Antoine, R.; Compagnon, I.; Rayane, D.; Broyer, M.; Dugourd, Ph.; Breaux, G.; Hagemester, F. C.; Phippen, D.; Hudgins, R. R.; Jarrold, M. F. *Eur. Phys. J. D* **2002**, *20*, 583.
- (5) Moro, R.; Rabinovitch, R.; Xia, C.; Kresin, V. V. *Phys. Rev. Lett.* **2006**, *97*, 123401.
- (6) Hertel, I. V.; Hüglin, C.; Nitsch, C.; Schulz, C. P. *Phys. Rev. Lett.* **1991**, *67*, 1767.
- (7) Schulz, C. P.; Bobbert, C.; Shimosato, T.; Daigoku, K.; Miura, N.; Hashimoto, K. *J. Chem. Phys.* **2003**, *119*, 11620.
- (8) Steinbach, C.; Buck, U. *J. Phys. Chem. A* **2006**, *110*, 3128.
- (9) Barnett, R. N.; Landman, U. *Phys. Rev. Lett.* **1993**, *70*, 1775.
- (10) Tsurusawa, T.; Iwata, S. *J. Phys. Chem. A* **1999**, *103*, 6134.
- (11) Ferro, Y.; Allouche, A. *J. Chem. Phys.* **2003**, *118*, 10461.
- (12) Gao, B.; Liu, Z. F. *J. Chem. Phys.* **2007**, *126*, 084501.
- (13) Buck, U.; Dauster, I.; Gao, B.; Liu, Z.-f. *J. Phys. Chem. A* **2007**, *111*, 12355.
- (14) Bobbert, C.; Schulz, C. P. *Eur. Phys. J. D* **2001**, *16*, 95.
- (15) Steinbach, C.; Buck, U. *J. Chem. Phys.* **2005**, *122*, 134301.
- (16) Bewig, L.; Buck, U.; Rakowsky, S.; Reymann, M.; Steinbach, C. *J. Phys. Chem. A* **1998**, *102*, 1124.
- (17) Ramsey, N. F. *Molecular Beams*; Clarendon Press: Oxford, UK, 1956, and references therein.
- (18) Aroney, M. J.; Pattern, S. J. *J. Chem. Soc., Faraday Trans.* **1984**, *80*, 1201.
- (19) Schäfer, S.; Heiles, S.; Becker, J. A.; Schafer, R. *J. Chem. Phys.* **2008**, *129*, 044304.
- (20) Rost, J. M.; Griffin, J. C.; Friedrich, B.; Herschbach, D. R. *Phys. Rev. Lett.* **1992**, *68*, 1299.
- (21) Benichou, E.; Allouche, A. R.; Antoine, R.; Aubert-Frecon, M.; Bourgoin, M.; Broyer, M.; Dugourd, Ph.; Hadinger, G.; Rayane, D. *Eur. Phys. J. D* **2000**, *10*, 233.
- (22) Dugourd, Ph.; Compagnon, I.; Lepine, F.; Antoine, R.; Rayane, D.; Broyer, M. *Chem. Phys. Lett.* **2001**, *336*, 511.
- (23) Bulthuis, J.; Becker, J. A.; Moro, R.; Kresin, V. V. *J. Chem. Phys.* **2008**, *129*, 024101.
- (24) Abd El Rahim, M.; Antoine, R.; Broyer, M.; Rayane, D.; Dugourd, Ph. *J. Phys. Chem. A* **2005**, *109*, 8507.
- (25) Dugourd, Ph.; Antoine, R.; Abd El Rahim, M.; Rayane, D.; Broyer, M.; Calvo, F. *Chem. Phys. Lett.* **2006**, *423*, 13.
- (26) Compagnon, I.; Antoine, R.; Rayane, D.; Broyer, M.; Dugourd, Ph. *J. Phys. Chem. A* **2003**, *107*, 3036.
- (27) Carrena, Á.; Mobbili, M.; Moriena, G.; Marceca, E. *Chem. Phys. Lett.* **2008**, *467*, 14.
- (28) Schäfer, S.; Schäfer, R. *Phys. Rev. B* **2008**, *77*, 205211.
- (29) Kittel, C. *Introduction to Solid State Physics*, 3rd ed.; Wiley: New York, 1967.
- (30) Farley, F. W.; McClelland, G. M. *Science* **1990**, *247*, 1572.
- (31) Rayane, D.; Antoine, R.; Dugourd, Ph.; Benichou, E.; Allouche, A. R.; Aubert-Frécon, M.; Broyer, M. *Phys. Rev. Lett.* **2000**, *84*, 1962.
- (32) Frisch, M. J.; Trucks, G. W.; Schlegel, H. B.; Scuseria, G. E.; Robb, M. A.; Cheeseman, J. R.; Zakrzewski, V. G.; Montgomery, J. A., Jr.; Stratmann, R. E.; Burant, J. C.; Dapprich, S.; Millam, J. M.; Daniels, A. D.; Kudin, K. N.; Strain, M. C.; Farkas, O.; Tomasi, J.; Barone, V.; Cossi, M.; Cammi, R.; Mennucci, B.; Pomelli, C.; Adamo, C.; Clifford, S.; Ochterski, J.; Petersson, G. A.; Ayala, P. Y.; Cui, Q.; Morokuma, K.; Malick, D. K.; Rabuck, A. D.; Raghavachari, K.; Foresman, J. B.; Cioslowski, J.; Ortiz, J. V.; Stefanov, B. B.; Liu, G.; Liashenko, A.; Piskorz, P.; Komaromi, I.; Gomperts, R.; Martin, R. L.; Fox, D. J.; Keith, T.; Al-Laham, M. A.; Peng, C. Y.; Nanayakkara, A.; Gonzalez, C.; Challacombe, M.; Gill, P. M. W.; Johnson, B. G.; Chen, W.; Wong, M. W.; Andres, J. L.; Head-Gordon, M.; Replogle, E. S.; Pople, J. A. *Gaussian 98*; Gaussian, Inc.: Pittsburgh, PA, 1998.
- (33) Sadlej, A. J. *Collect. Czech. Chem. Commun.* **1988**, *53*, 1995.
- (34) Ekstrom, C. R.; Schmiedmayer, J.; Chapman, M. S.; Hammond, T. D.; Pritchard, D. E. *Phys. Rev. A* **1995**, *51*, 3883.
- (35) Yang, M.; Senet, P.; Van Alsenoy, C. *Int. J. Quantum Chem.* **2005**, *101*, 535.
- (36) Ghanty, T. K.; Ghosh, S. K. *J. Chem. Phys.* **2003**, *118*, 8547.
- (37) Rodriguez, J.; Laria, D.; Marceca, E.; Estrin, D. *J. Chem. Phys.* **1999**, *110*, 9039.
- (38) Klots, C. E. *J. Phys. Chem.* **1988**, *92*, 5864.
- (39) Hashimoto, K.; Morokuma, K. *J. Am. Chem. Soc.* **1994**, *116*, 11436.